

## Supplementary Data S1

### Over-expression of *GPAT9* in *Arabidopsis* increases seed oil content and alters the fatty acid composition of seed oil

Constitutive over-expression of the *GPAT9* coding sequence in *Arabidopsis* resulted in a small but significant 2.8% relative increase in oil content on a per weight basis in T<sub>2</sub> transgenic seeds compared to wild type (Fig. S4A). To ascertain that any changes in lipid production in transgenic seeds were not a result of phenotypic alterations in vegetative or floral tissues, we also produced lines that over-expressed *GPAT9* in a seed-specific manner (GPAT9-SS-OE; Fig. S1). As was the case for the constitutive GPAT9-OE lines (Fig. S2), over-expression of *GPAT9* was confirmed in developing siliques (14 DAF) from a selection of T<sub>1</sub> GPAT9-SS-OE lines via quantitative real-time RT-PCR, whereby *GPAT9* transcripts were detected at levels enhanced by 682.4% to 3137.7% compared to wild-type levels (Fig. S8A). As was the case for T<sub>2</sub> GPAT9-OE seeds, T<sub>2</sub> GPAT9-SS-OE seeds also exhibited a small but significant 3.0% relative increase in oil content compared to wild-type seeds (Fig. S4B).

To further verify these changes in seed oil content in *GPAT9* over-expression lines, T<sub>3</sub> seeds from two homozygous GPAT9-OE lines with confirmed over-expression of *GPAT9* were similarly analyzed. Interestingly, while oil content analyses of these lines demonstrated small relative increases in seed oil content as a percentage of weight (1.6% and 2.9%, respectively), these changes were not significant (Fig. S5A); a result which could possibly be attributed to the relatively small sample size of T<sub>3</sub> homozygous plants compared to T<sub>2</sub> lines and the inherent variability of seed oil content in *Arabidopsis*, which can make detecting statistically valid changes in oil content difficult (Li et al. 2006). However, due to the increase in seed size in GPAT9-OE lines, when seed oil content was measured on a per seed basis rather than on a per weight basis, a significant increase in mean oil content was noted in both transgenic lines, corresponding to 11.7% (GPAT9-OE-6) and 12.2% (GPAT9-OE-7) relative increases compared to wild-type plants (Fig. S5B).

Significant alterations in the FA composition of seed oil from both GPAT9-OE and GPAT9-SS-OE lines were also evident. Overall, the seed oil of transgenic lines exhibited reductions in 20:1, as well as increases in 18:1, and 22:0 (Fig. S4 and Fig. S5C).

## **Down-regulation of *GPAT9* in Arabidopsis decreases seed oil content and alters the fatty acid composition of seed oil**

Constitutive down-regulation of *GPAT9* in Arabidopsis using RNAi resulted in a significant 5.3% relative decrease in oil content on a per weight basis in T<sub>2</sub> transgenic seeds compared to wild type (Fig. S6A). Similarly, seed-specific *GPAT9*-SS-RNAi lines (Fig. S1), where *GPAT9* transcripts were reduced in T<sub>1</sub> developing siliques (14 DAF) in a selection of lines by between 32.3% and 29.6% compared to wild-type levels (Fig. S9B), exhibited a significant 8.9% relative decrease in oil content compared to wild-type lines (Fig. S6B).

To provide further verification of these reductions in seed oil content in *GPAT9* RNAi lines, we also analyzed lipids from T<sub>3</sub> seeds from two independent homozygous *GPAT9*-RNAi lines with confirmed down-regulation of *GPAT9*. As was the case for both constitutive *GPAT9*-RNAi and seed-specific *GPAT9*-SS-RNAi T<sub>2</sub> seeds, oil content analyses of *GPAT9*-RNAi T<sub>3</sub> seeds demonstrated a significant decrease in seed oil content (relative decreases of 7.3% and 4.2% for *GPAT9*-RNAi-10 and *GPAT9*-RNAi-21 lines, respectively, compared to wild type) as a percentage of weight (Fig. S7A). Similarly, when seed oil content was measured on a per seed basis rather than on a per weight basis, even greater decreases in mean oil content were noted in both transgenic lines, corresponding to 20.6% (*GPAT9*-RNAi-10) and 8.0% (*GPAT9*-RNAi-21) relative reductions compared to wild-type lines (Fig. S7B).

Significant alterations in FA composition of the seed oil of both *GPAT9*-RNAi and *GPAT9*-SS-RNAi lines were also evident. Overall, the seed oil of transgenic lines exhibited reductions in 16:0, 18:2, 20:1, 22:0 and 22:1 FAs, as well as increases in 18:0, 18:1, and 18:3 (Fig. S6 and Fig. S7C).

## **References**

**Li Y, Beisson F, Pollard M, Ohlrogge J.** 2006. Oil content of Arabidopsis seeds: the influence of seed anatomy, light and plant-to-plant variation. *Phytochemistry* 67, 904-915.

1 **Supplemental figures**

2

3 **Title: Arabidopsis GPAT9 contributes to synthesis of intracellular glycerolipids but not**  
4 **surface lipids**

5

6 **Authors:**

7 Stacy D. Singer <sup>1,\*</sup>, Guanqun Chen <sup>1,\*</sup>, †, Elzbieta Mietkiewska<sup>1</sup>, Pernell Tomasi <sup>2</sup>, Kethmi  
8 Jayawardhane <sup>1</sup>, John M. Dyer<sup>2</sup>, and Randall J. Weselake <sup>1, §</sup>

9

10 **Figure S1:** Quantitative real-time RT-PCR analysis of Arabidopsis *GPAT9* expression

11 **Figure S2:** Schematic representations of experimental plant transformation constructs.

12 **Figure S3:** Confirmation of alterations in *GPAT9* expression in siliques from GPAT9-OE and  
13 GPAT9-RNAi homozygous lines compared to wild type.

14 **Figure S4:** Seed weight and seed area in homozygous GPAT9-OE, GPAT9-RNAi and wild-type  
15 lines.

16 **Figure S5:** Oil content and fatty acid composition of T<sub>2</sub> GPAT9-OE, GPAT9-SS-OE and wild-  
17 type seeds.

18 **Figure S6:** Seed oil content and composition in homozygous T<sub>3</sub> GPAT9-OE and wild-type lines.

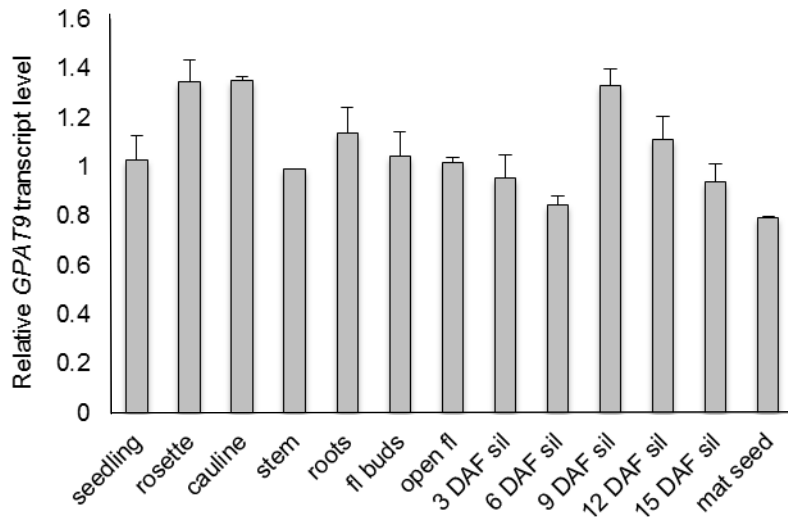
19 **Figure S7:** Oil content and fatty acid composition of T<sub>2</sub> GPAT9-RNAi, GPAT9-SS-RNAi and  
20 wild-type seeds.

21 **Figure S8:** Seed oil content and composition in homozygous T<sub>3</sub> GPAT9-RNAi and wild-type  
22 lines.

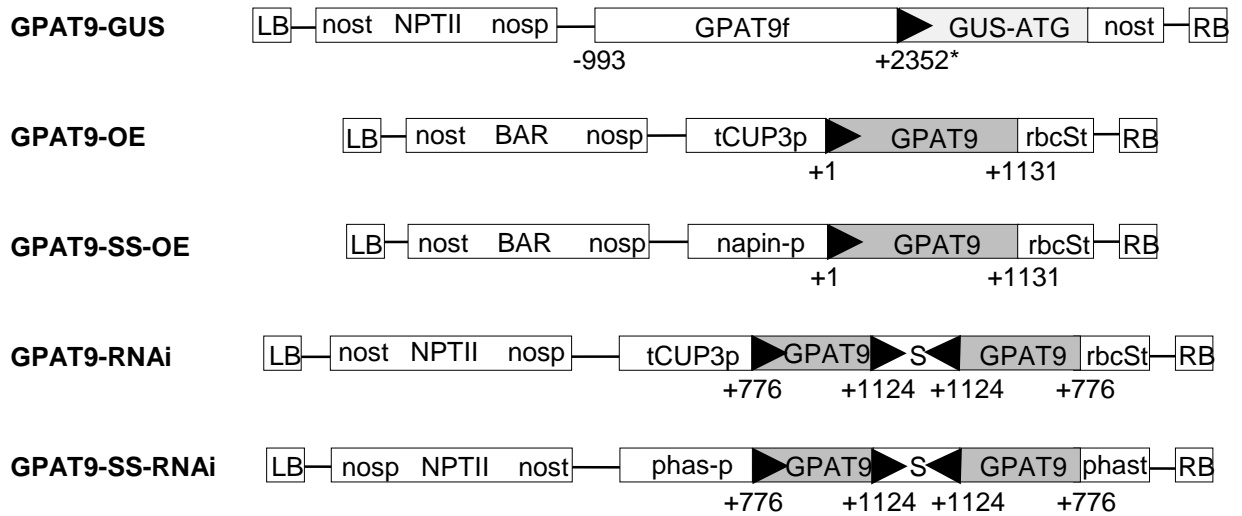
23 **Figure S9:** Growth rates of GPAT9-OE, GPAT9-RNAi and wild-type seedlings.

24 **Figure S10:** Confirmation of alterations in *GPAT9* expression in GPAT9-SS-OE and GPAT9-SS-  
25 RNAi lines compared to wild type.

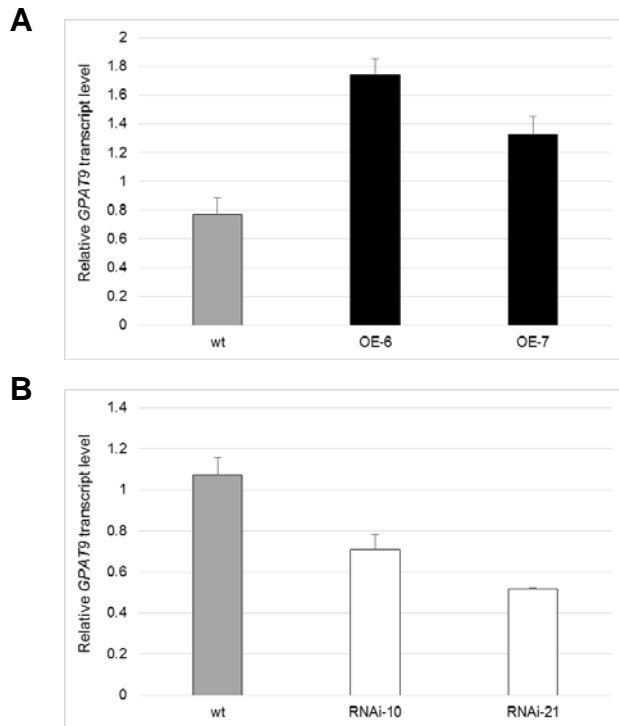
26



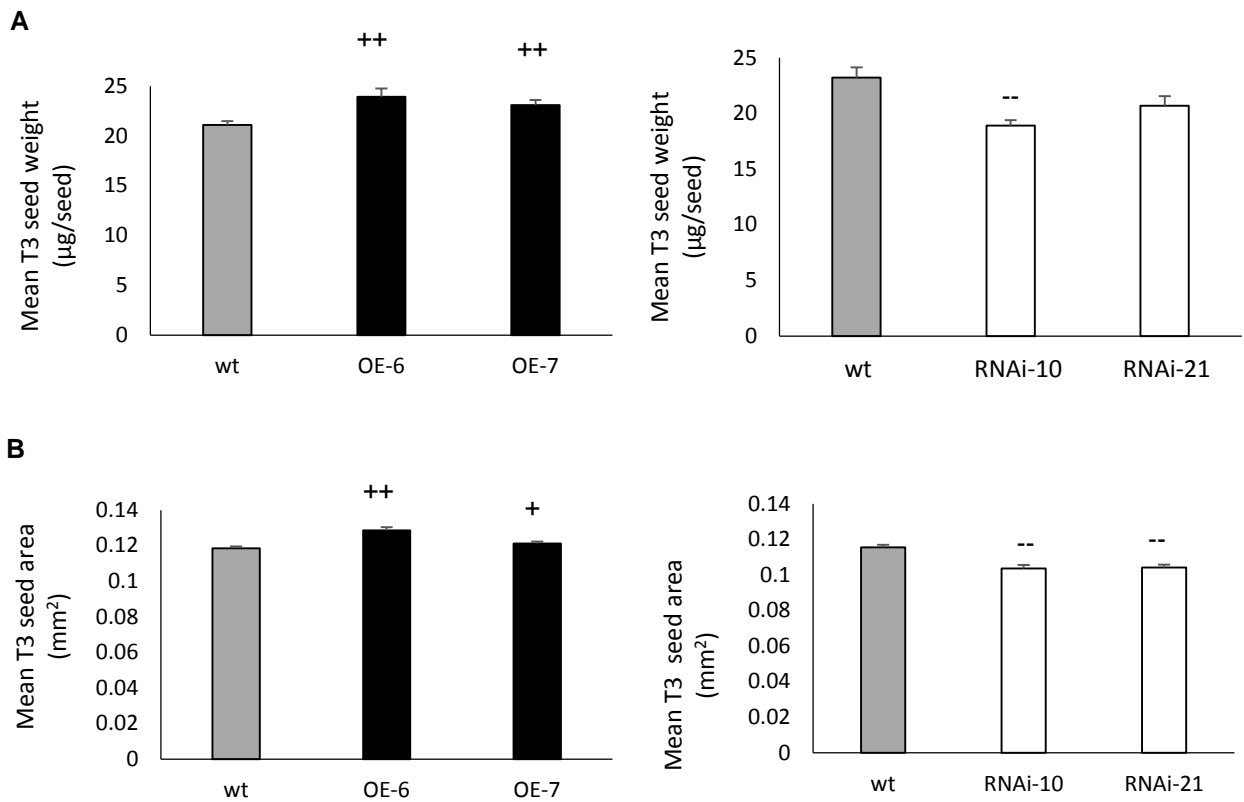
**Fig. S1.** Arabidopsis *GPAT9* expression analyses with quantitative real-time RT-PCR analysis of Arabidopsis Col-0 tissues at numerous developmental stages. Three technical replicates were carried out in each case. Blocks represent the mean *GPAT9* transcript level of two biological replicates relative to levels of the internal control transcript, *PP2AA3*. Bars denote standard errors. DAF, days after flowering; fl, flower; mat, mature; sen, senescing; sil, siliques.



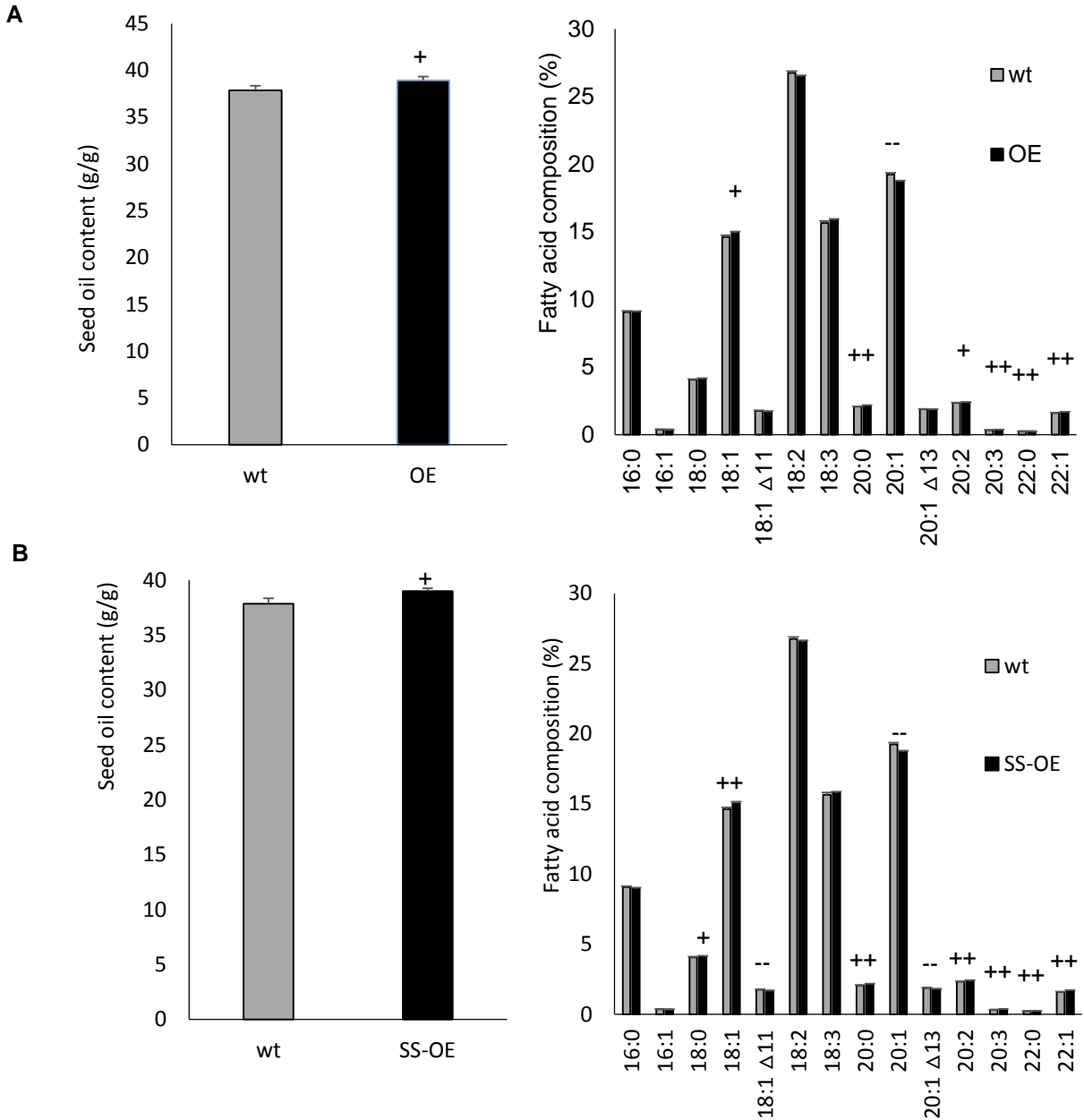
**Fig. S2.** Schematic representations (not to scale) of experimental plant transformation constructs utilized in this study. Numbers indicate nucleotides relative to the Arabidopsis *GPAT9* start codon (+1). Numbers within the GPAT9-GUS vector representation denote nucleotides of genomic sequence, while those of the remaining vectors indicate coding sequence. Arrows indicate the direction of transcription in each case. BAR, phosphinothricin acetyltransferase; GPAT9, Arabidopsis *GPAT9* sequence; LB, left T-DNA border; napin-p, *Brassica napus* *Napin* promoter; nosp, *Nopaline synthase* promoter; nost, *Nopaline synthase* transcriptional terminator; NPTII, *Neomycin phosphotransferase II*; phas-p, *Phaseolus vulgaris* *Phaseolin* promoter; phast, *Phaseolin* transcriptional terminator; RB, right T-DNA border; rbcSt, *Pisum sativum* *Ribulose-1,5-bisphosphate carboxylase* transcriptional terminator; S, intronic spacer; tCUP3p, tobacco *tCUP3* constitutive promoter.



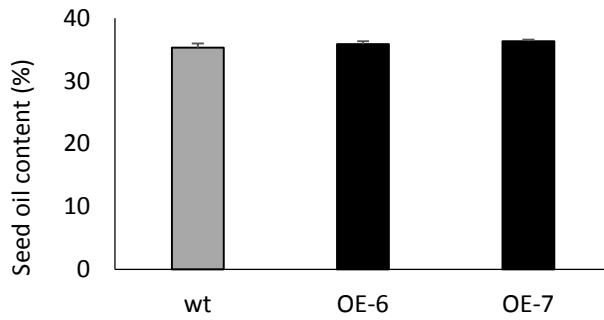
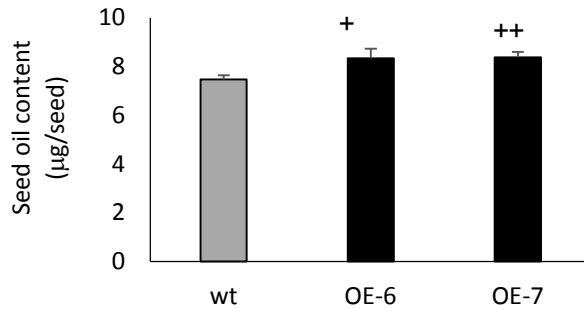
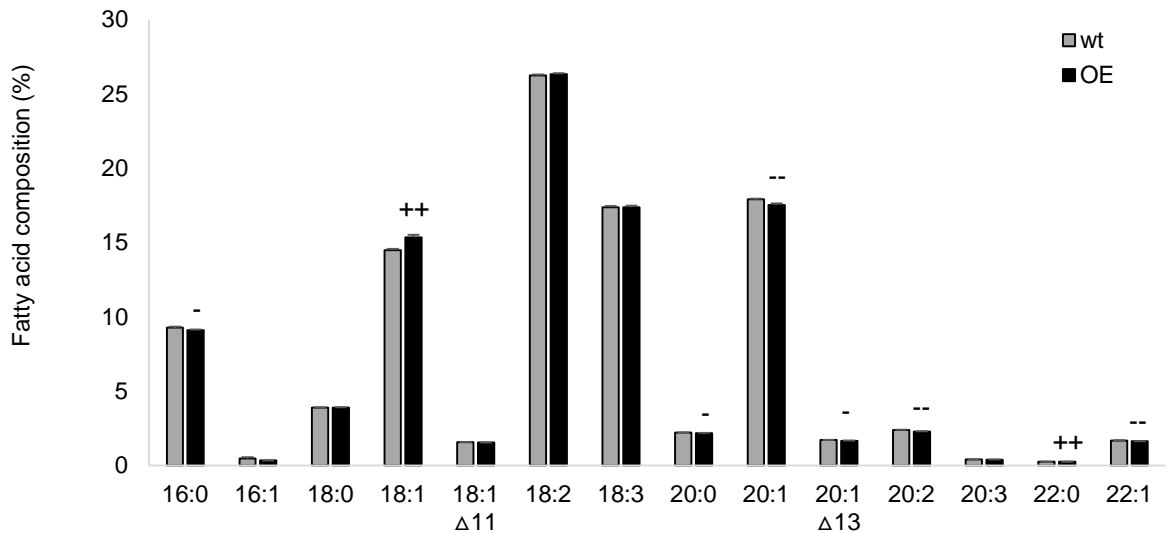
**Fig. S3.** Confirmation of alterations in *GPAT9* expression in siliques from *GPAT9*-OE and *GPAT9*-RNAi homozygous lines compared to wild type. Quantitative real-time RT-PCR analysis of *GPAT9* expression in homozygous T<sub>2</sub> siliques (14 DAF) from *GPAT9*-OE (**A**), *GPAT9*-RNAi (**B**) and wild-type lines. Three technical replicates were carried out in each case. Blocks denote mean *GPAT9* transcript levels from three biological replicates relative to the internal control, *PP2AA3*, and bars indicate standard errors.



**Fig. S4.** Seed weight and seed area in homozygous GPAT9-OE, GPAT9-RNAi and wild-type lines. A, Seed weights of  $T_3$  homozygous lines. Blocks indicate mean weights of seeds from wild-type ( $n=14$ ), OE-6 ( $n=5$ ), OE-7 ( $n=7$ ); wild-type ( $n=15$ ), RNAi-10 ( $n=5$ ), and RNAi-21 ( $n=7$ ) lines, with three technical replicates measured in each case. B, Seed areas of  $T_3$  homozygous lines. Blocks indicate mean areas of wild-type ( $n=113$ ), OE-6 ( $n=65$ ), OE-7 ( $n=107$ ); wild-type ( $n=127$ ), RNAi-10 ( $n=59$ ), and RNAi-21 ( $n=81$ ) seeds. In all instances, bars denote standard errors. Significant increases and decreases compared to wild type (as measured by Student's t-test) are indicated by +/++ ( $P \leq 0.05/P \leq 0.01$ ) and -- ( $P \leq 0.01$ ). OE, GPAT9-OE lines, RNAi, GPAT9-RNAi lines, wt, wild type.



**Fig. S5.** Oil content and fatty acid composition of T<sub>2</sub> GPAT9-OE, GPAT9-SS-OE and wild-type seeds. A, Mean seed oil content and fatty acid composition in GPAT9-OE lines. Blocks represent mean values of wild-type ( $n=14$ ) and GPAT9-OE ( $n=15$ ) independent lines. B, Mean seed oil content and fatty acid composition in GPAT9-SS-OE lines. Blocks indicate mean values of wild-type ( $n=14$ ) and GPAT9-SS-OE ( $n=15$ ) independent lines. Two technical replicates were carried out for every line analyzed. Bars denote standard errors. Significant increases and decreases compared to wild type (as measured by Student's t-test) are indicated by +/++ ( $P \leq 0.05/P \leq 0.01$ ) and - - ( $P \leq 0.01$ ). OE, GPAT9-OE; SS-OE, GPAT9-SS-OE; wt, wild type; TFA, total fatty acid.

**A****B****C**

**Fig. S6.** Seed oil content and composition in homozygous  $T_3$  GPAT9-OE and wild-type lines. A, Seed oil content on a per weight basis. B, Seed oil content on a per seed basis. In the case of oil content analyses, blocks represent mean values from wild-type ( $n=14$ ), GPAT9-OE-6 ( $n=5$ ) and GPAT9-OE-7 ( $n=7$ ) lines. C, Fatty acid composition of seed oil. In the case of fatty acid composition, blocks represent the mean values of wild-type and pooled GPAT9-OE-6 and GPAT9-OE-7 lines. Bars denote standard errors. Significant increases and decreases compared to wild type (as measured by Student's t-test) are indicated by +/++ ( $P \leq 0.05/P \leq 0.01$ ) and -/- ( $P \leq 0.05/P \leq 0.01$ ). OE, GPAT9-OE; wt, wild type.

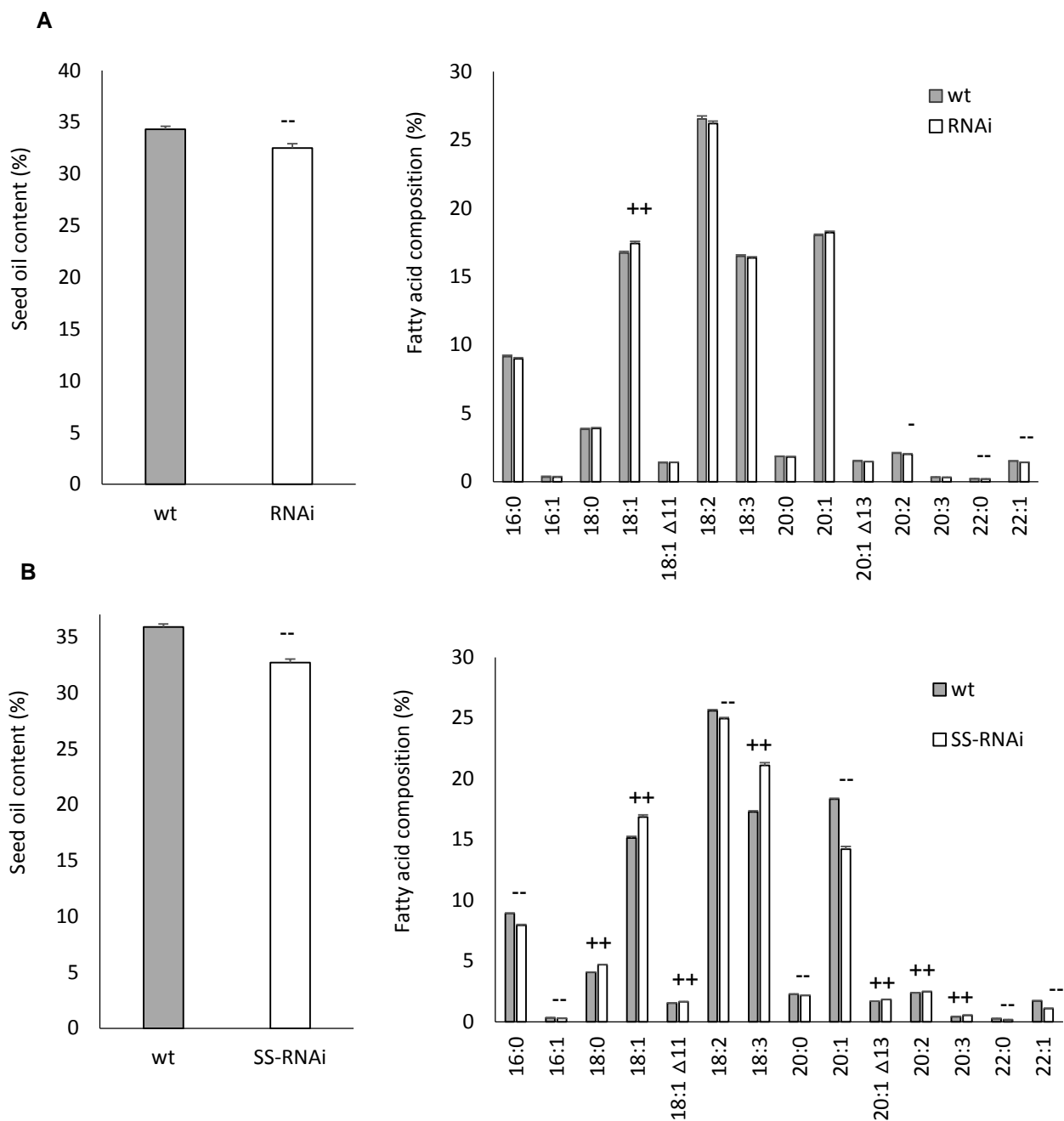


**Fig. S7.** Oil content and fatty acid composition of  $T_2$  GPAT9-RNAi, GPAT9-SS-RNAi and wild-type seeds. A, Mean seed oil content and fatty acid composition in GPAT9-RNAi lines. Blocks represent mean values of wild-type ( $n=16$ ) and GPAT9-RNAi ( $n=29$ ) independent lines. B, Mean seed oil content and fatty acid composition in GPAT9-SS-RNAi lines. Blocks indicate mean values of wild-type ( $n=25$ ) and GPAT9-SS-RNAi ( $n=25$ ) independent lines. Two technical replicates were carried out for every line analyzed. Bars denote standard errors. Significant increases and decreases compared to wild type (as measured by Student's t-test) are indicated by ++ ( $P \leq 0.01$ ) and -/- ( $P \leq 0.05/P \leq 0.01$ ). RNAi, GPAT9-RNAi; SS-RNAi, GPAT9-SS-RNAi; wt, wild type; TFA, total fatty acids.

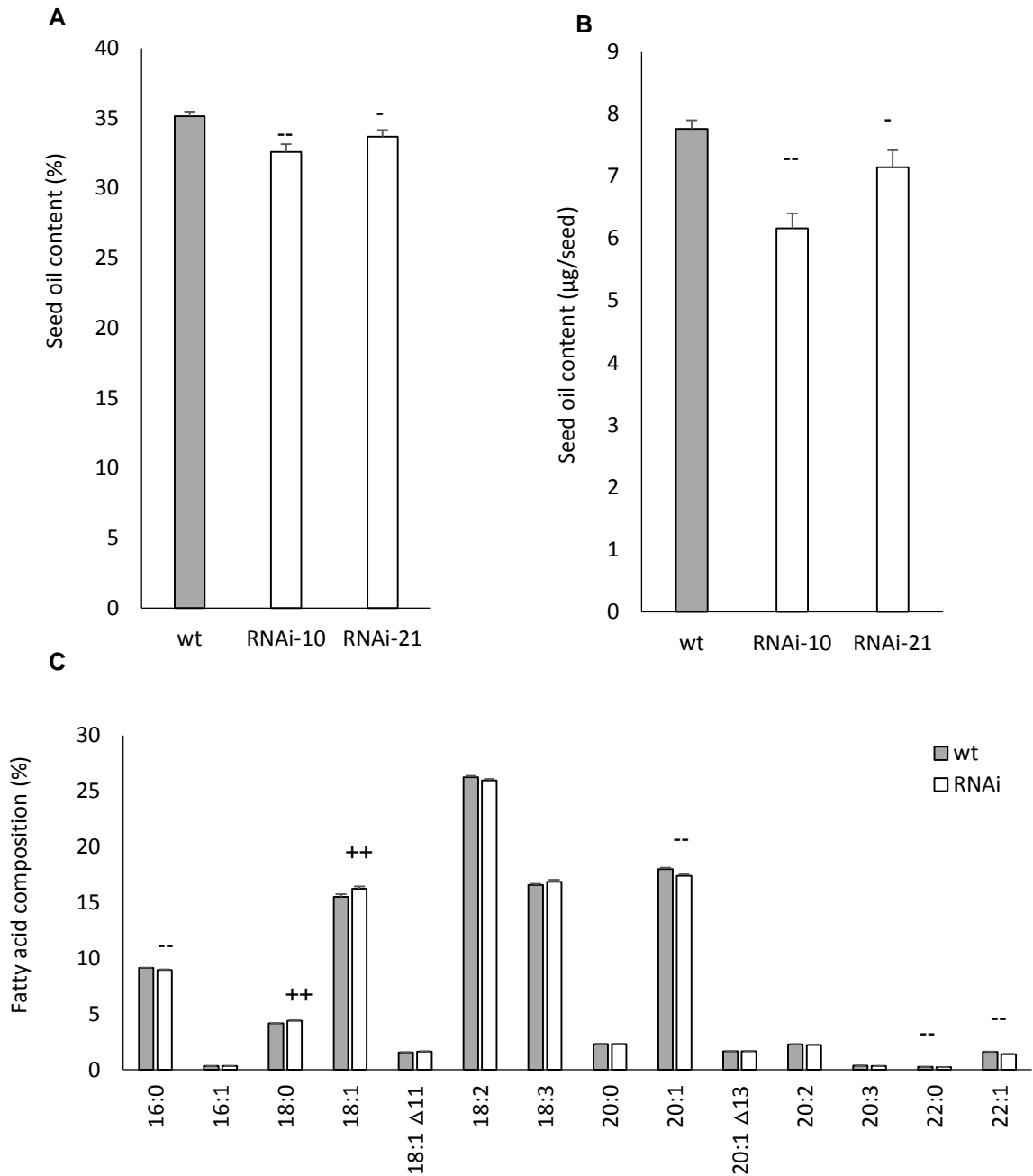


**Fig. S8.** Seed oil content and composition in homozygous T<sub>3</sub> GPAT9-RNAi and wild-type lines. A, Seed oil content on a per weight basis. B, Seed oil content on a per seed basis. In the case of oil content, blocks represent mean values from wild-type ( $n=15$ ), GPAT9-RNAi-10 ( $n=5$ ) and GPAT9-RNAi-21 ( $n=7$ ) lines. C, Fatty acid composition of seed oil. In the case of fatty acid composition, blocks represent the mean values of wild-type and pooled GPAT9-RNAi-10 and GPAT9-RNAi-21 lines. Bars denote standard errors. Significant increases and decreases compared to wild type (as measured by Student's t-test) are indicated by ++ ( $P \leq 0.01$ ) and -/- - ( $P \leq 0.05/P \leq 0.01$ ). RNAi, GPAT9-RNAi; wt, wild type; TFA, total fatty acids.

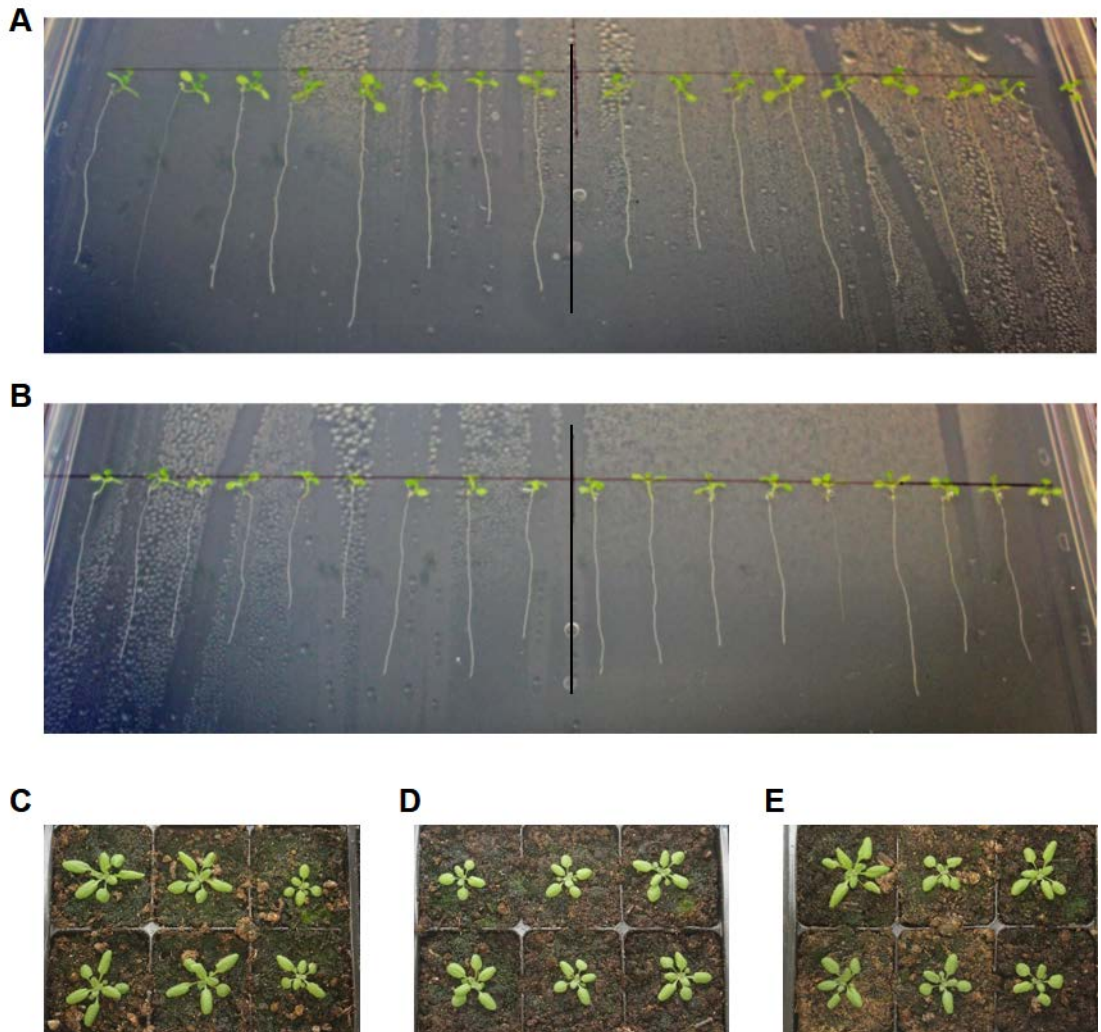


**Fig. S9.** Growth rates of GPAT9-OE, GPAT9-RNAi and wild-type seedlings. (A and B) Seedlings grown vertically on solid medium were photographed 15 days post-germination and are representative of two independent experiments. GPAT9-OE (A) and GPAT9-RNAi (B) seedlings are shown to the left of the black line, while wild-type seedlings are present to the right in both instances. (C-E) Soil grown wild-type (C), GPAT9-OE (D) and GPAT9-RNAi (E) lines 17 days post-germination.

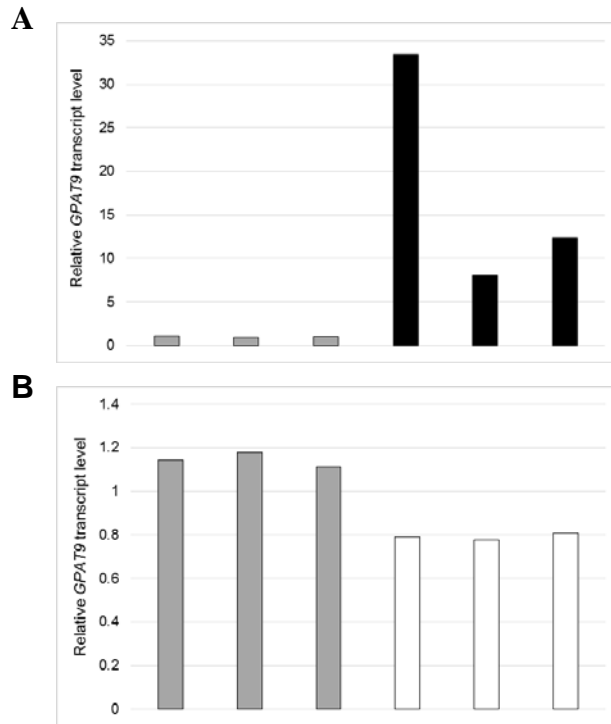


**Fig. S10.** Confirmation of alterations in *GPAT9* expression in GPAT9-SS-OE and GPAT9-SS-RNAi lines compared to wild type. Quantitative real-time RT-PCR analysis of *GPAT9* expression in T<sub>1</sub> siliques (14 DAF) from independent GPAT9-SS-OE (**A**), GPAT9-SS-RNAi (**B**) and wild-type lines. Blocks denote mean *GPAT9* transcript levels from three technical replicates relative to the internal control, *PP2AA3*. Gray blocks represent wild-type plants, black blocks represent independent GPAT9-SS-OE lines, and white blocks represent independent GPAT9-SS-RNAi lines.